technologies

MDPI

Article

Prosthetic Hand Based on Human Hand Anatomy Controlled by Surface Electromyography and Artificial Neural Network

Larisa Dunai [1,*], Isabel Seguí Verdú [1], Dinu Turcanu [2] and Viorel Bostan [2]

[1] Department Graphical Engineering, Universitat Politècnica de Valencia, 46022 Valencia, Spain; issever@doctor.upv.es
[2] Department of Software Engineering and Automatics, Technical University of Moldova, MD-2004 Chisina, Moldova; dinu.turcanu@adm.utm.md (D.T.); viorel.bostan@adm.utm.md (V.B.)
* Correspondence: ladu@upv.es

Abstract: Humans have a complex way of expressing their intuitive intentions in real gestures. That is why many gesture detection and recognition techniques have been studied and developed. There are many methods of human hand signal reading, such as those using electroencephalography, electrocorticography, and electromyography, as well as methods for gesture recognition. In this paper, we present a method based on real-time surface electroencephalography hand-based gesture recognition using a multilayer neural network. For this purpose, the sEMG signals have been amplified, filtered and sampled; then, the data have been segmented, feature extracted and classified for each gesture. To validate the method, 100 signals for three gestures with 64 samples each signal have been recorded from 2 users with OYMotion sensors and 100 signals for three gestures from 4 users with the MyWare sensors. These signals were used for feature extraction and classification using an artificial neuronal network. The model converges after 10 sessions, achieving 98% accuracy. As a result, an algorithm was developed that aimed to recognize two specific gestures (handling a bottle and pointing with the index finger) in real time with 95% accuracy.

Keywords: prosthetic hand; bionic hand; EMG; gesture recognition; feature extraction; classification

check for updates

Academic Editors: Frédéric C. Lebon and Ahmad Lotfi

Received: 26 September 2024
Revised: 13 December 2024
Accepted: 31 December 2024
Published: 2 January 2025

Citation: Dunai, L.; Verdú, I.S.; Turcanu, D.; Bostan, V. Prosthetic Hand Based on Human Hand Anatomy Controlled by Surface Electromyography and Artificial Neural Network. *Technologies* **2025**, *13*, 21. https://doi.org/10.3390/technologies13010021

Copyright: © 2025 by the authors. Licensee MDPI, Basel, Switzerland. This article is an open access article distributed under the terms and conditions of the Creative Commons Attribution (CC BY) license (https://creativecommons.org/licenses/by/4.0/).

1. Introduction

Globally, over 3 million people live with hand amputations [1], significantly impacting their independence and daily functionality. Various prosthetic hands are available on the market to improve quality of life, though many remain inaccessible due to high costs. Prosthetic hands can be categorized into several types: passive prostheses, which are purely cosmetic and serve no functional purpose, and body-powered prostheses, which use mechanical systems operated by cables connected to the user's body. Bionic hands represent the most advanced option, enabling hand movement through the use of actuators and signals derived from electromyography (EMG), electroencephalography (EEG), or electrocorticography (ECoG). Among these, EMG-based bionic hands show the most promise [2]. EMG-based bionic hands utilize surface electromyography (sEMG) sensors placed on the residual forearm to detect muscle activity, converting these signals into functional hand movements. The use of EMG for prosthetic control dates back to 1957, initially for simple ON/OFF control of DC motors [3]. Today, EMG signals enable a range of control mechanisms, including ON/OFF switching, proportional control, pattern recognition control, and posture control. The development of bionic hands aims to provide

users with intuitive, easy-to-control prostheses that offer more natural movements. Within the bionic hand market, various manufacturers provide models with distinct features. These systems generally rely on hand-coded control mechanisms. For example, co-contraction control systems use two channels, allowing users to switch between functions generated for each channel.

Several notable models include the Sensor Hand from Otto Bock, which features two active fingers for gripping, and more advanced systems like the Michelangelo [3,4], BeBionic [5], Sensor Hand [6–8], i-Limb [9] from Touch Bionics, and Vincent Hand [10,11] from Vincent Systems, all of which incorporate five active fingers for more natural dexterity. These models are controlled via sEMG sensors and are optimized for dexterous grasping functionality. Each model employs different control strategies. For instance, the i-Limb uses double and triple impulses for hand control, while the BeBionic employs co-contractions and offers multiple wrist options, including an EQD (electric quick disconnect) wrist, a short wrist for longer residual limbs, and a flexion wrist. The Vincent Hand relies on switch signals, co-contractions, and double impulses. The Sensor Hand utilizes muscle contractions for hand control and a slip-detection method for force control [12].

Table 1 summarizes the key characteristics of various sEMG-based prosthetic hands.

Table 1. Comparison of EMG prosthetic hands.

Model	Developer	DOF	Control Type	N Fingers	Grip Patterns	Costs
Michelangelo	Otto-Bock	2	Co-contractions	5	7	USD 73,800
Be Bionic	Otto-Bock	6	Co-contractions	5	14	USD 5200
Sensor Hand	Otto-Bock	1	Co-contractions	3	6	USD 1500.00
i-Limb	Össur	6	Double and triple-impulse	5	36	USD 33,443.20
Vincent Hand	VINCENT Systems	6	Switch signal, co-contractions, double impulse	5	4	USD 50,000.00

The most common approach in real-world prosthetics involves the use of myoelectric prostheses, primarily controlled by EMG signals from the amputee's residual limb. However, EEG and ECoG signals originating from the brain are also viable control methods. There are several examples of prosthetic hand control using EEG [13] and ECoG [14]. Since these control methods are non-invasive, they are primarily applied in clinical and research settings. Sensors, such as EMG, are placed on the skin of the amputee's residual limb to detect nerve signals, or in the case of ECoG, brain signals, which are processed by electronic systems to enable hand movements. However, the consistency of surface EMG signal acquisition can be compromised by slight variations in electrode placement between different sessions. Standardizing electrode positioning is challenging due to the unique muscular structure of each individual [15].

sEMG signal acquisition relies on active analog sensors [12] that incorporate discrete components for comprehensive analog signal conditioning. These sensors include band-pass filters, differential instrumentation amplifiers, and feedback circuits for motor offset removal. While these sensors offer high signal-to-noise ratios and effective noise cancellation, they are expensive and typically housed in large, cumbersome units. This design constraint presents challenges for developing cost-effective, scalable, and compact prosthetic systems, as expanding the number of input channels necessitates additional analog circuitry, thereby increasing system cost and size.

To address these limitations, advanced signal processing techniques have been developed to improve the decoding of movement signals from the human body to the prosthetic hand. This includes the use of biomimetic sensors that provide detailed information during prosthesis operation. Additionally, sensory feedback systems have been created to replicate sensations such as movement, touch, and even pain, thereby enhancing the user's interac-

tion with the prosthetic limb [16]. These innovations in prosthetic technology aim to make artificial limbs more functional and lifelike, offering users improved control and sensory feedback [17]. Continued advancements in this field are expected to yield even more sophisticated prosthetic devices, further improving the quality of life and independence of amputees.

EMG signals are particularly advantageous as they enable finer detection of muscle activity, allowing for more complex movements. In this context, the integration of Artificial Intelligence (AI) into EMG signal processing has great potential. Neural networks, for instance, could significantly enhance the accuracy of EMG signal analysis, reducing the need for multiple sensors and simplifying the system architecture [18].

Despite the promising advancements, Artificial Intelligence (AI) in prosthetic control systems still faces several limitations [19]. First, AI systems require extensive learning databases, necessitating numerous acquisitions for each desired movement. While this process is crucial for achieving high accuracy, it is time-consuming and labor-intensive. Additionally, the effects of muscle fatigue and atrophy in amputees can introduce substantial variability compared to data from healthy individuals, further complicating the learning process. Selecting the appropriate output neurons is another challenge, as it requires careful decisions about which movements will be individually recognized, and which should be grouped together. Moreover, executing AI algorithms demands more powerful and, consequently, more expensive electronic components.

Given the progress in commercial and experimental prosthetic devices, there remain significant areas for improvement. One persistent issue is data acquisition. Factors such as the placement and shifting of EMG electrodes on the arm, varying skin conditions, the weight of the prosthesis, and the disparity between the prosthetic's trained data and the signals generated by the user all pose challenges to the performance of current bionic hands. The use of advanced algorithms alone does not necessarily enhance device functionality.

This work presents a simplified training algorithm for functional detection, utilizing neural networks and Kalman filters. The proposed algorithms are straightforward to implement and can reliably detect hand grips through simple muscle contractions. This approach offers a practical solution for improving responsiveness and ease of control in prosthetic hands, making the technology more accessible and user-friendly.

2. System Description

The proposed system in this paper introduces a multifunctional acquisition and processing platform, focusing on the design, hardware, and software development of a prosthetic hand for detecting and classifying hand grips and gestures.

The design of the prosthetic hand is primarily guided by user needs and the ergonomic principles of human anatomy [20]. Medical devices must meet strict criteria for adaptability and user customization. In the case of hand prostheses, tailoring a device for each individual user is often impractical due to the inherent variability in human anatomy. To address this challenge, our approach focuses on creating a universal prosthesis design that can be easily adapted to suit different users. By designing components based on average anthropometric data, we can ensure that the prosthesis is both functional and customizable. The system is designed to allow parameterization, enabling adjustments to individualize the device for each user without requiring a complete redesign.

Ergonomic considerations also extend beyond function to user acceptance, which includes aesthetics as a key factor. Aesthetics play a crucial role in user comfort and device acceptance, which many prosthetic designs often overlook. To address this, our prosthetic hand is covered with a flesh-colored silicone layer that mimics the appearance of a natural human hand. This layer conceals the mechanical components, giving the prosthesis a more

lifelike and non-intimidating appearance, which is crucial for enhancing user experience and social confidence.

The prosthesis is not only designed with functional requirements in mind but is also modeled closely after human hand anatomy. Each phalanx was 3D scanned from a real human hand, and the prosthetic components were then precisely 3D-printed to replicate the natural structure. Additionally, ligaments and nerve pathways were recreated to mimic the intricate dynamics of the human hand, as shown in Figure 1 [20]. This detailed anatomical modeling ensures that the prosthetic hand provides both the functional dexterity and the aesthetic realism necessary for improving the user's quality of life.

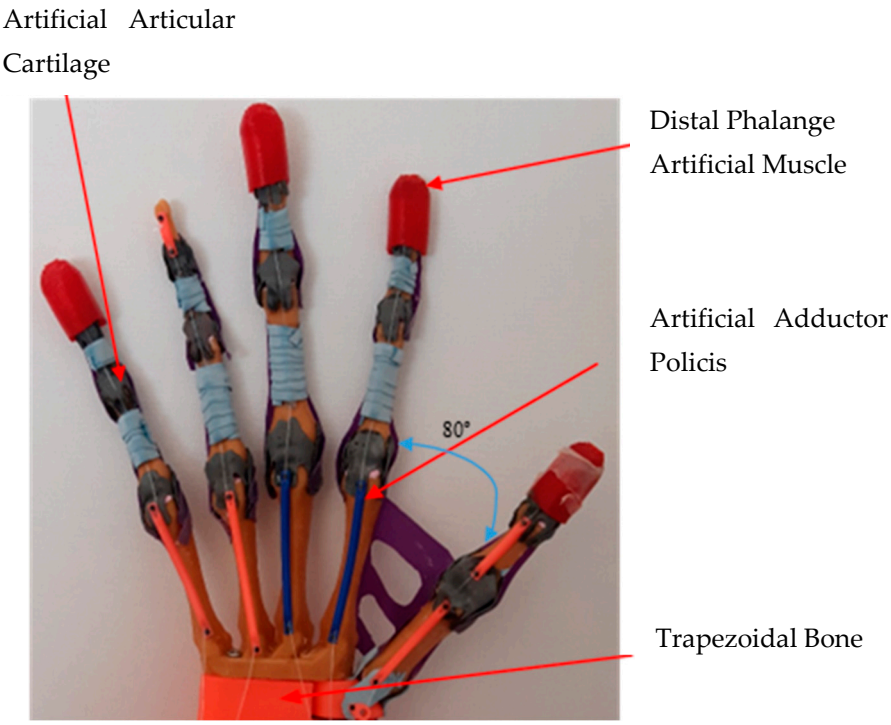

Figure 1. Mechanical assembly of the prosthetic hand [20].

For the design of the prosthetic hand, the physical properties of the materials used were carefully analyzed. The phalanges were fabricated from a photopolymer resin, chosen for its specific mechanical properties, including a temperature resistance range of 15 °C to 35 °C, a hardness of 80–85D, flexural strength between 30–50 MPa, flexural modulus of 700–1000 MPa, and tensile strength of 30–48 MPa. The control system for the prosthetic hand consists of an ESP32 microcontroller, three OYMotion surface EMG sensors, five stepper motors and controllers to facilitate flexion and extension movements, a servo motor for thumb abduction, and five force sensors.

The current version of the prosthetic hand operates primarily in the sagittal plane. The motivation behind developing a new bionic hand is to create a design based on the natural anatomy of the human hand and phalanges, which will allow for more natural movements and reduce the risk of lateral damage to the phalanges. In this design, key anatomical features of the human hand are incorporated: volar plates are positioned on the palm side to connect the phalanges and prevent hyperextension; collateral ligaments are integrated to secure the joints and allow for controlled flexibility and abduction between phalanges. The extensor hood, a structure that facilitates natural extension, is replicated in the design to ensure smooth extension of the fingers, while a flexor tendon system is employed to replicate finger flexion.

This advanced design achieves a more accurate imitation of human hand movements compared to existing bionic prostheses. By incorporating these anatomical features, the bionic hand offers more natural and fluid movements, making it a significant improvement over traditional designs in terms of both function and biomechanical accuracy.

2.1. Surface EMG Control System and Preprocessing

Surface Electromyography (sEMG) is employed in the proposed system to perform two key functions: (1) ON/OFF control, and (2) control of prosthetic hand and finger movements, as depicted in Figure 2. The sEMG sensors capture neuronal electrical signals transmitted to the hand muscles, which encode specific commands for different movements. Sartori et al. [21] developed a model-based decoder capable of synthesizing musculoskeletal dynamics, and similarly, our system is controlled by EMG signals from the residual limb.

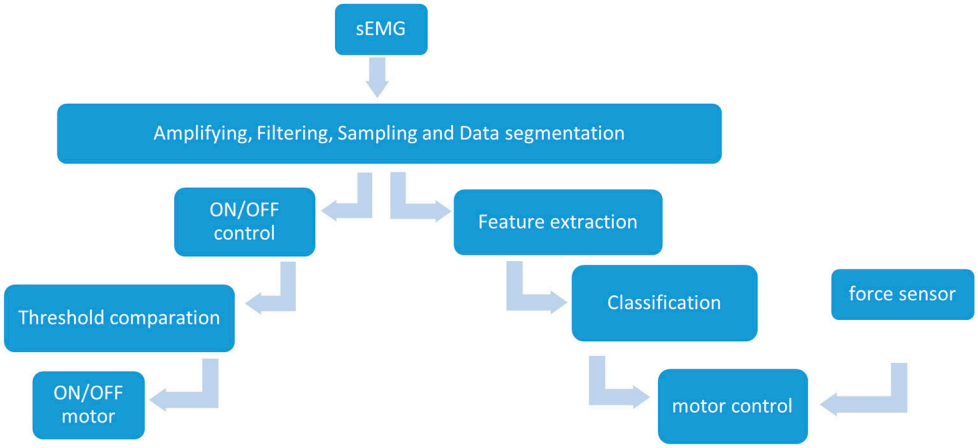

Figure 2. Surface EMG prosthetic hand control system.

It is important to note that while the extracted signals in this study are obtained from healthy individuals with fully functional arms, the situation differs for individuals with hand amputations. In amputees, some muscles may become inactive over time, limiting the number of muscles available for signal acquisition. The time elapsed since the amputation is another critical factor; if the amputation occurred recently, the brain still sends neural signals to the residual muscles, and the muscles remain active. However, in cases where a significant amount of time has passed, the brain may reduce or stop sending motor signals to the amputated area. The signal characteristics also differ in congenital amputees, where the brain has never sent motor commands for hand movements. Amputees often produce lower-intensity, less-defined signals, particularly in higher-level amputations, due to compensating for missing muscles. This reduction in signal quality is a consequence of the limited number of active muscle fibers contributing to the sEMG signals. Also, amputees show more variability in sEMG signals due to individual adaptations and variations in muscle activation patterns [22]. Over time, amputees may develop unique muscle control patterns, altering the characteristics of their EMG signals. Prosthetic control algorithms for amputees face increased difficulty due to lower signal specificity and higher variability, often requiring advanced processing methods. While EMG signals from amputees can be used for prosthesis control, they typically require more advanced processing techniques to achieve reliable outcomes that is why gesture recognition for prosthetic hand control is usually used by healthy users. For this reason, gesture recognition algorithms are often trained using data from healthy individuals, as their sEMG signals are more consistent and easier to process. This allows for initial algorithm validation before transitioning to amputee-specific datasets, which involve additional complexities.

The ON/OFF control mechanism is based on detecting sEMG signals from the residual upper limb muscles and comparing them to a predefined threshold. This allows the prosthetic hand to start or stop functioning. Previous studies [1,20] demonstrated that this method effectively controlled grip function in prosthetic hands, with the sEMG signals serving as indicators of movement intention. Additionally, force sensors integrated into the hand measure the grip pressure applied to objects, providing precise control.

To enhance natural hand function, a secondary control system based on pattern recognition is incorporated into the prosthetic device. This system uses algorithms for pattern recognition and classification to identify and classify hand movements from sEMG signals. The pattern recognition process includes feature extraction and classification of the sEMG data, allowing for more intuitive and responsive control of the prosthetic hand. By analyzing the information extracted from the sEMG signals, this method enables the prosthetic hand to mimic natural hand movements more accurately.

OYMotion EMG sensors and Sparkfun MyoWare sensors (Figure 3) are used to control the prosthetic arm. The characteristics of both sensors can be seen in Table 2. The OyMotion sEMG features a metal surface instead of single-use electrodes like MyoWare ones. The OyMotion sEMG amplifies the signal to transform the input signal of ± 1.5 mV to an output signal between 0 V and 3 V. The MyoWare sEMG requires filters to filter the RAW EMG signals.



Figure 3. The surface OYMotion and Sparkfun MyoWare EMG sensors.

Table 2. Technical data of the Sparkfun MyWare AT-04-001 and OYMotion sEMG sensors.

	MyWare	**OyMotion**
Supply voltage	+3.3–5.7 V	+3.3–5.5 V
Operating Voltage	+3.3 V	+3 V
Detection Range	-	$+/-$ 1.5 mV
Current supply	14 mA	20 mA
Spectrum Range	10–400 Hz	20–500 Hz
Output modes	EMG Envelope/Raw EMG	Analog

In typical applications, surface electromyography (sEMG) signals are commonly acquired from the biceps brachii and triceps brachii muscles. This conventional placement is advantageous for prosthetic systems that extend from the hand to the elbow, as it allows for external sensor application without the need for internal integration. In our study, however, we have strategically positioned the sEMG sensors on the extensor digitorum and extensor carpi radialis brevis muscles. This choice facilitates seamless integration of the sensors into the prosthetic device rather than solely aiming for optimal signal fidelity.

For thumb abduction control, a dedicated sensor is placed on the abductor pollicis longus muscle, as depicted in Figure 4. While the extensor digitorum muscle governs the movement of all fingers except the thumb, maintaining appropriate spacing between the sensors is critical. This spacing is essential as it defines the signal bandwidth necessary for effective filtering, thereby enhancing the clarity and quality of the captured data.

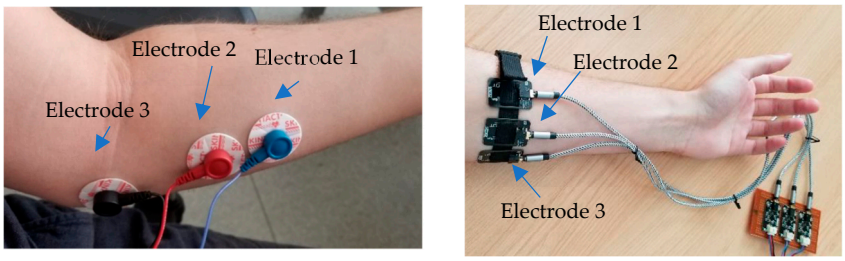

Figure 4. Sensor placement for data collection for both MyWare AT-04-001 and OYMotion sEMG sensors.

Optimal sensor placement is vital to ensure that sEMG signals are acquired from distinct muscle groups without cross-interference. In configurations utilizing multiple sensors—such as our three-sensor arrangement—mixing of signals can occur, which may compromise the reliability of the output. To address this challenge, we employ advanced signal processing techniques designed to isolate and refine mixed signals. This methodological approach ensures accurate and reliable control of the prosthetic hand, ultimately enhancing its functionality, responsiveness, and overall user experience.

Surface electromyography (sEMG) sensors are employed to capture the electrical signals generated by muscle activity. However, the recorded signals often include extraneous information that may not contribute meaningfully to pattern recognition and classification tasks. Additionally, incorporating a larger number of sensors to gather more data can be counterproductive, as each additional channel may introduce redundancy and increase processing complexity, thereby elevating computational costs. Research by Hahne et al. has demonstrated that employing a limited number of channels can optimize system performance, reducing both the computational resources and training data required for effective operation.

To enhance the efficacy of the sEMG sensors, the acquired signals are subjected to band-pass filtration, adhering to Kirchhoff's Law for Sparkfun MyoWare sensors. The signals must be filtered with a band-pass filter and after that the signals must be rectified and again with the low-pass filter to smooth the envelope.

The Sparkfun MyoWare signals were filtered with:

$$y[n] = a * x[n] + (1 - a) * y[n - 1] \tag{1}$$

where a = 0.3.

These filters are specifically designed to isolate frequency components within the range of 20 Hz (f1) to 150 Hz (f2), which are crucial for accurately capturing relevant muscle activity.

The OYMotion sensors have the frequency band from 50 to 150 Hz, so the cut-off frequencies were chosen at 20 Hz and 150 Hz and the anti-hum filter is a notch filter centered on 50 Hz. Because both filters are at a sampling frequency of 500 Hz, the signal is rectified using the sq (square) function. This rectified signal is then filtered for the last time using a simple first-order digital filter with coefficient α = 0.03 as can be seen in the formula given by the sensor developer below.

$$\mathrm{HLPF(z)} = \frac{(0.3913 + 0.7827\mathrm{z}^{-1} + 0.3913\mathrm{z}^{-2})}{(1 + 0.3695\mathrm{z}^{-1} + 0.1958\mathrm{z}^{-2})} \tag{2}$$

$$\mathrm{HHPF(z)} = \frac{(0.8371 - 1.6742\mathrm{z}^{-1} + 0.8371\mathrm{z}^{-2})}{(1 - 1.6475\mathrm{z}^{-1} + 0.7009\mathrm{z}^{-2})} \tag{3}$$

$$\mathrm{HAHF}(z) = \frac{(0.9522 - 1.5407z^{-1} + 0.9522z^{-2} + 0.8158z^{-3} - 0.8045z^{-4} + 0.0855z^{-5})}{(1 - 1.5395z^{-1} + 0.9056z^{-2} + z^{-3} - 1.1187z^{-4} + 0.3129z^{-5}} \quad (4)$$

The envelope of the EMG signal is then obtained. The envelope is extremely stable and reliable, and there is significantly less noise from OYMotion sEMG compared to the MyoWare sEMG sensor.

Given that muscle signals transition from a resting state to contraction and back to rest, the time-domain signals are truncated to concentrate on the essential phases of muscle activation. This focused approach improves the clarity and relevance of the recorded signals, facilitating more accurate analysis and interpretation within the context of pattern recognition and classification, ultimately enhancing the functionality of prosthetic control systems.

2.2. Data Segmentation and Sampling

Once the signals have been recorded and filtered, the subsequent phase entails signal segmentation, which is essential for extracting relevant information from the data and enabling effective feature extraction. In this study, we utilize an adjacent windowing technique, where the windows do not overlap.

The purpose of windowing is to isolate specific segments of the entire input signal that contain critical information required for analysis. An optimal window size is determined for both signal sampling and feature extraction processes. In this research, a window size of 100 ms has been established, as illustrated in Figure 5. This duration is selected based on empirical evidence indicating that signals exhibit enhanced accuracy during the initial 100 ms, making it particularly advantageous for classification tasks.

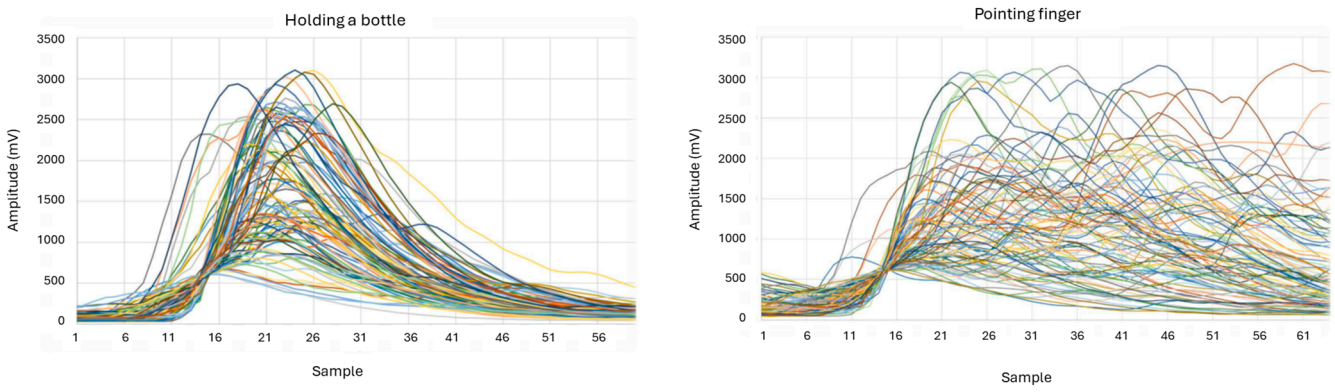

(**a**) (**b**)

Figure 5. 100 sEMG signal recording for (**a**) handling a bottle and (**b**) pointing finger. Each color represents a signal for the same gesture.

The windowing mechanism is dynamic and continuously advances, capturing and storing new data in real time. This approach ensures that the most pertinent and timely information is obtained, thereby facilitating more precise and efficient analysis in subsequent processing stages.

To define the best sEMG sensors for data collection, two types of typologies were used: the MyoWare and OYMotion surface sensors. It can be observed from Figure 6 that the signal-to-noise ratio of OYMotion sensors is significantly higher than that of MyoWare sensors.

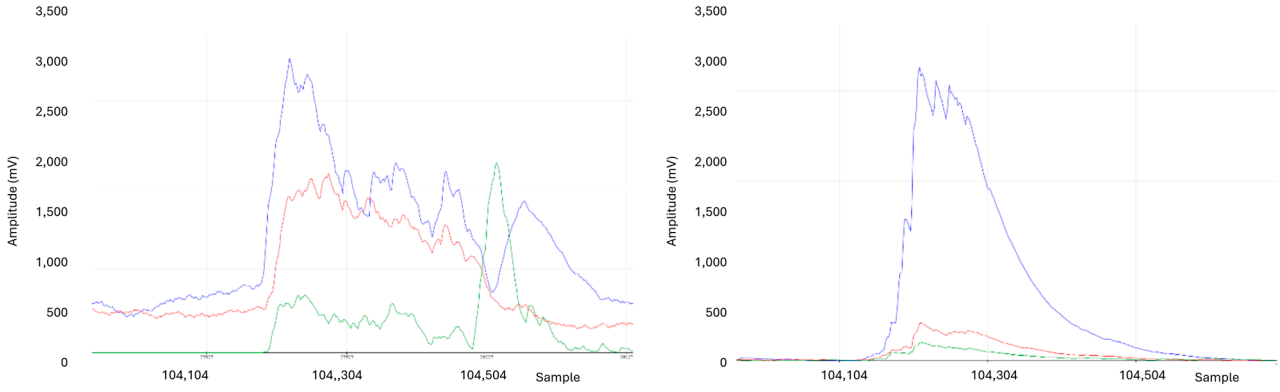

Figure 6. Comparison of the filtered signals from Sparkfun sensors and surface OYMotion EMG sensors. (**a**) Sparkfun MyoWare sEMG sensor; (**b**) OYMotion sEMG sensors. Each color represents the signals from the three sensors used for Sparkfun MyoWare and three for OYMotion sensors. The green line is from sensor 3, the red is from sensor 1, and the blue is from sensor 2. The position of the three sensors can be seen in Figure 4.

This fact was also observed by Hudgins in [23,24]. Since myoelectric signals can exhibit unpredictable behavior during transitions between different levels of muscle contractions, classification errors frequently arise when switching between classes. To address this issue, short segment lengths have been employed for signal classification. The data segments that belong to the transition period are eliminated. This process improves the data used for the training process because only the needed signals are used, removing the residual signals.

2.3. Feature Extraction

Following the filtering and sampling of the surface electromyography (sEMG) signals, feature extraction is implemented to facilitate analysis. Feature extraction methods can be classified into several categories: Time Domain (TD), Frequency Domain (FD), Time-Frequency Domain (TFD), Integral Absolute Value (IAV), and Mean Relative Value (MRV).

To validate the operational effectiveness of the system, a database was established using a single sensor comprising 100 acquisitions for two distinct movements: "holding a bottle" and "pointing the index finger." Each acquisition consists of 64 samples collected at 10 ms intervals, 10 samples preceding the signal edge and 54 samples following it. An initial program was developed in C/C++ utilizing the Arduino IDE to create this database. This program directs the microcontroller to continuously monitor its analog input connected to the sEMG sensor. When the detected signal exceeds a predetermined threshold, the microcontroller transmits the 64 signal samples to a computer via the serial port.

The individual wearing the electrodes is instructed to perform each movement, enabling the collection of a comprehensive database stored in a CSV file for subsequent training purposes. The database comprises a separate CSV file for each movement type, with each file containing 100 acquisitions and 64 voltage samples per acquisition. Figure 7 presents graphical representations of the databases created for the "holding a bottle" and "pointing finger" movements using a single sensor.

This structured methodology ensures systematic data collection and organization for each movement, thereby providing a robust dataset for subsequent analysis and machine learning training. The repetition of movements by the subject, coupled with the consistent sampling by the microcontroller, is crucial for capturing the variability and nuances of the EMG signals associated with each specific action. This approach establishes a solid foundation for developing accurate models to interpret and predict muscle activity based on sEMG data.

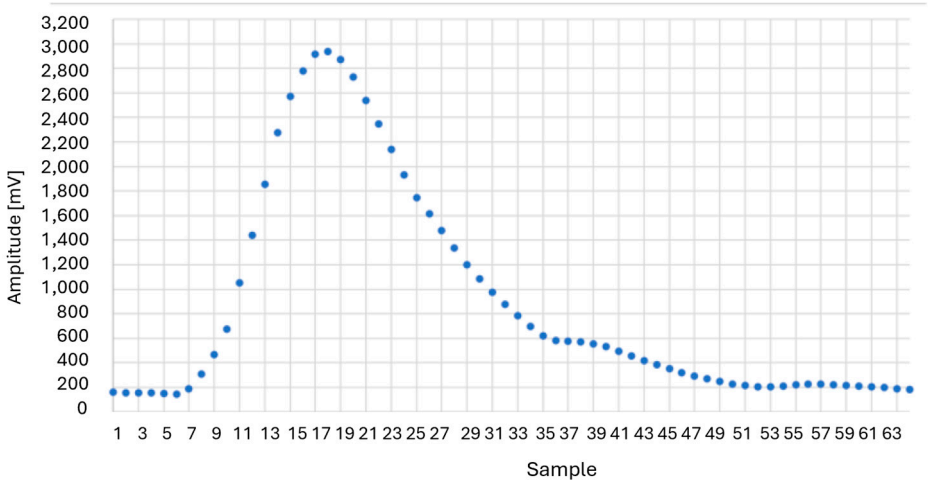

Figure 7. The 64 signals acquired with the sEMG used for the Artificial Neuronal Network process.

2.4. Signal Classification

Signal classification entails the efficient categorization of preprocessed signals. A plethora of studies have demonstrated the effectiveness of multi-layer perceptron and neural network architectures for the extraction and classification of multiple finger features. Traditional classification techniques employed in this domain include support vector machines (SVM) [25], linear discriminant analysis (LDA) [26], Bayesian analysis, fuzzy logic (FL) [27], k-nearest neighbors (KNN) [28], and hidden Markov models (HMM) [29]. Additionally, recent advancements in the field have introduced more contemporary methods, such as artificial neural networks (ANN) [30] and convolutional neural networks (CNN), alongside significant progress in deep learning frameworks.

Each classification approach proves effective in categorizing the extracted feature space, yet they exhibit unique characteristics attributed to the intrinsic differences in their underlying algorithms. In reference [31], Short-Time Fourier Transform (STFT) is employed for feature extraction and classification. In contrast, reference [32] utilizes neural network algorithms incorporating deep learning techniques, such as ANN and recurrent neural networks (RNN). In the time-domain (TD) approach, features are derived based on signal amplitude and temporal parameters.

The Artificial Neural Network designed for this study consists of an input layer that processes 192 signal samples (64 samples from each of the three sensors). This input layer is followed by a hidden layer containing 64 neurons, a subsequent layer with 128 neurons, and a dropout layer implemented to mitigate overfitting. Following this, another hidden layer with 64 neurons is succeeded by an additional three layers with 64 neurons each. The final output layer comprises two neurons, each representing a distinct type of movement.

For the study, we used TensorFlow Keras Sequential model that reads and processes one input tensor to one output tensor. We used ReLu that will pass the list of layers to the Sequential constructor.

The accuracy of the system was calculated using the following formula:

$$Accuracy = \frac{TP + TN}{TP + TN + FP + FN} * 100\%$$

where TP is the true positive rate, TN is the true negative rate, FN is false negatives and FP is false positives.

To optimize the model's performance, we employ the Adam optimizer from Keras, as proposed by Professor Andrew Ng [33]. This optimizer effectively reduces instances of underfitting and overfitting, thereby enhancing the overall training process, as illustrated

in Figure 8. The Categorical Crossentropy loss function is utilized, given that our labels are formatted in a one-hot encoded manner. Additionally, convolutional models are implemented for the comprehensive evaluation of classification performance, ensuring a robust assessment of the proposed method's efficacy.

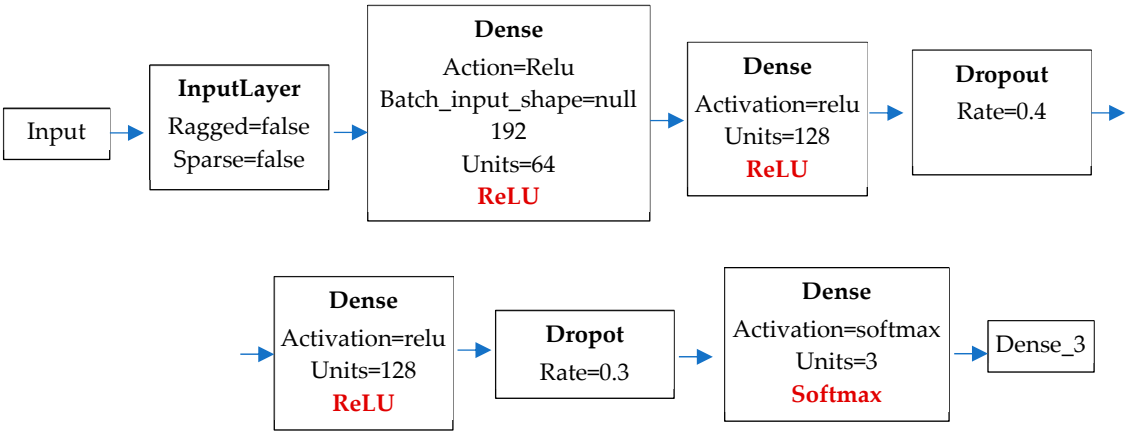

Figure 8. Neural Network used for the three sensors.

To address underfitting in the ANN, its architecture was expanded by either increasing the number of layers or adding neurons within each layer. Additionally, the training duration was extended by increasing the number of epochs, providing the ANN more iterations to converge effectively. Once satisfactory accuracy was achieved on the training dataset, measures to mitigate overfitting were implemented. These modifications were carefully implemented to ensure that the model could learn sufficient features from the input data without overburdening the computational resources of the microcontroller.

Regularization techniques, such as the inclusion of dropout layers, were employed to encourage the ANN to generalize by simulating the absence of certain information during training. The dropout rate was adjusted based on the number of neurons in the affected layer, with higher dropout values assigned to layers with a larger neuron count. Nonlinear activation functions, including sigmoid, tanh, and ReLU (as illustrated in Figure 8), were applied to neurons to introduce nonlinearity into their responses, enhancing the network's ability to model complex patterns. Lastly, the dataset size was increased to provide the ANN with more diverse training examples, further enhancing its efficiency and generalization capability. During the testing phase of the ANN, dropout rates were systematically evaluated to optimize accuracy. In this study, dropout rates were set to 0.4 and 0.3, meaning 40% of the neurons in the first layer and 30% of the neurons in the second layer were randomly deactivated by setting their outputs to zero. This approach mitigates overfitting by compelling the network to learn more generalized and robust features, reducing dependency on specific neurons and improving the overall model performance. The dropout rates of 0.4 and 0.3 were chosen after iterative testing, where various dropout combinations were evaluated for their impact on accuracy and generalization. Although an ablation study was not conducted specifically, the selected rates align with those commonly reported in the literature for networks of similar size and complexity [34].

Addressing underfitting and overfitting is critical for optimizing training performance. This can be achieved by fine-tuning the batch size, which determines the number of samples used for weight updates during training. In scenarios where the dataset size is relatively small, it is advisable to use the maximum batch size, equal to the total number of available acquisitions, to fully utilize the dataset. The learning rate and learning rate decay, which dictate the step size during each iteration of parameter updates, were carefully configured. A lower learning rate ensures more precise convergence but may increase

training time. Normalizing the input values between 0 and 1, to maintain small magnitudes, can further enhance training performance by improving numerical stability during model computations. However, this normalization introduces additional computational overhead on resource-constrained devices, such as microcontrollers, as each input acquisition would require a division operation during inference. This trade-off between training performance and inference efficiency must be carefully considered, particularly when deploying the neural network on low-power embedded systems.

A double-trigger mechanism has been implemented to augment the system's versatility while maintaining simplicity in the artificial intelligence architecture. This mechanism enables the bionic hand to execute an alternative action upon the detection of a repeated movement akin to a double-click action. By leveraging this approach, the system is capable of classifying and recognizing six distinct commands, thereby allowing the bionic hand to perform a total of six unique movements. This enhancement not only improves the functional repertoire of the prosthetic device but also streamlines user interactions by facilitating intuitive control options.

To optimize hardware processing, TinyML was utilized, an emerging field that integrates embedded systems with machine learning (ML) [35]. TinyML facilitates the deployment of ML models on devices with limited computational resources, enabling real-time, on-device decision-making without constant cloud connectivity. This is particularly advantageous for applications such as gesture recognition [36], voice command processing [37], image or video analysis, and environmental monitoring in IoT and sustainability initiatives.

The TinyML deployment process involves data collection from hardware equipped with an inference engine [38]. This data is either stored locally or imported into tools like Edge Impulse Studio for model training. The trained ML model is then converted to TensorFlow Lite (TFLite) format, optimized for microcontroller units (MCUs), and exported as a C-byte array for deployment [39]. On the MCU, the TinyML library ensures efficient deployment by using an OpResolver API, which specifies necessary network operations and minimizes firmware size [40]. A dedicated memory block, the "arena," is allocated for intermediate computations, managed by the TFLite Interpreter. This setup enables local data processing with low latency and high efficiency.

TinyML's ability to deploy robust ML models on resource-limited devices enhances real-time inference and decision-making, ensuring responsive and efficient operation without extensive computational resources.

3. Results

Experimental results demonstrate the feasibility of classifying three distinct movements: "clench fist", "wrist extension", and "wrist flexion". These movements exhibit significant differences, leading to the generation of clear and distinguishable surface electromyography (sEMG) signals, as illustrated in Figure 9. Notably, visual inspection reveals a pronounced distinction between the signals corresponding to "wrist flexion" and "wrist extension," highlighting the efficacy of the classification methodology employed in this study.

Upon analyzing the signals depicted in Figure 9, it becomes apparent that the movements "wrist flexion" and "clench fist" exhibit considerable similarity due to the overlapping activation of the two primary muscles responsible for these actions in the forearm. This overlap leads to classification errors when attempting to differentiate between "wrist flexion" and "clench fist". Furthermore, in the context of everyday movements, the distinctions between similar actions, such as "clench fist" versus "pinch", and "pointing finger" versus "click on a mouse", are often minimal. Taking into consideration the sensor placements in Figure 9, we can observe that sensors 1 and 2 detect movements for wrist flexion and

clenched fists. For wrist flexion, there were no signals, or it was so small that it was not detected. For the wrist extension, the signal was detected by the 3rd sensor.

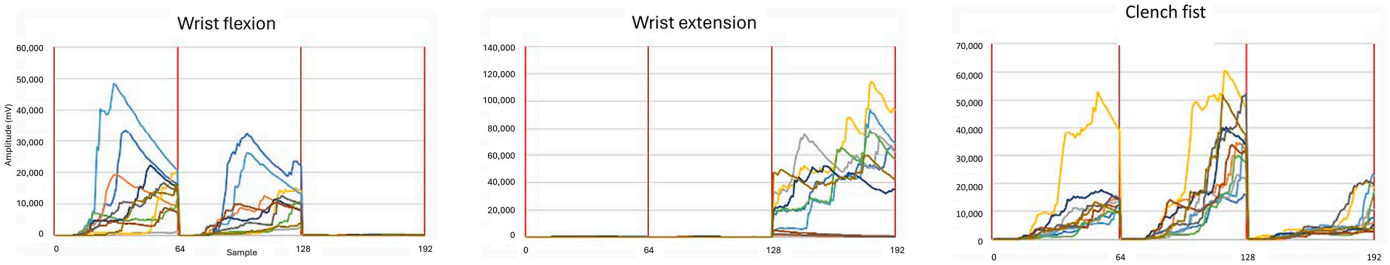

Figure 9. Three simple movement signals (one sensor per column). A color represents each recorded signal. Each column represents the three sensors for wrist flexion, wrist extension and clench fist: 1st column represents the 1st sensor, 2nd column is the 2nd sensor, and 3rd column is the 3rd sensor. Ten signals were captured with all three sensors for all three movements.

To address this challenge, the median signals for each movement are represented in Figure 10. Notably, for Sensor 1, the median signals corresponding to the five movements display significant confusion, indicating that the placement of Sensor 1 during data acquisition may have been suboptimal. This observation suggests that careful sensor positioning is critical for enhancing classification accuracy in muscle movement recognition.

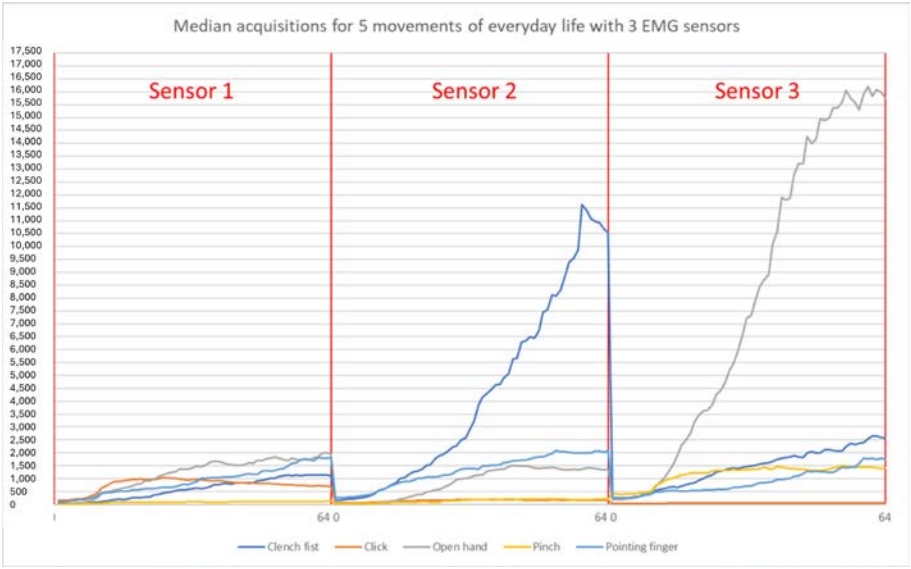

Figure 10. Median acquisition for five movements: clench fist, click, open hand, pinch and pointing finger of everyday life with three sEMG sensors. Each movement is presented with a specific color that can be seen in the figure caption.

For Sensors 2 and 3, it is evident that the signals corresponding to the movements "clench fist" and "open hand" exhibit clear differentiation, primarily attributed to their distinct amplitude profiles. Also, it can be perceived that for these two movements, as an example the clench fist, the signal is received by the 2nd sensor and has fewer signals recorded from 1 and 3. In contrast, sensor 3 recorded a great signal for the open hand movement, but sensors 1 and 2 had a small signal. However, as illustrated in the mean deviation plot presented in Figure 11, the variability in the mean deviation is substantial. This significant deviation is indicative of an unreliable signal, suggesting that the amplitude fluctuates considerably based on factors such as the force exerted during the movement and the positional orientation of the wrist. Such variability underscores the need for improved

signal stabilization methods to enhance the reliability of muscle movement classification. On the analysis of the "clench fist" movement, Figure 11 illustrates that the mean deviation is comparable in magnitude to the median signal. Specifically, an examination of the final samples recorded by Sensor 2 reveals a striking disparity: the weakest recorded amplitude for the "clench fist" movement is 82, while the strongest measures an astonishing 80,710, representing a difference of nearly 1000-fold.

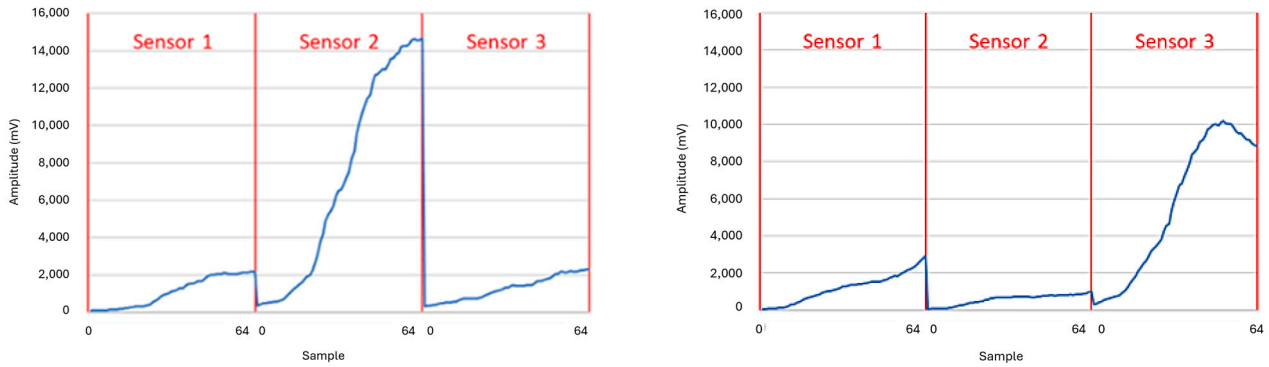

(**a**) (**b**)

Figure 11. Graphical representation of the mean signals recorded by the three sensors for clench fist and open hand gestures. (**a**) Mean deviation of "clench fist" signal; (**b**) Mean deviation of "open hand" signal for the three sEMG sensors recorded by the three OyMotion sEMG sensors.

This substantial variability in amplitude measurements presents a significant challenge, undermining the potential for reliable and robust learning within artificial intelligence systems. Such pronounced discrepancies hinder the model's ability to generalize effectively across the range of input signals, thereby limiting classification accuracy and overall performance.

The results demonstrate that the model performs exceptionally well across all classes, with an overall accuracy of 98.26% and a weighted F1-score of 0.98, as seen in Table 3. The metrics highlight the following:

- The "Wrist Extension" class achieved perfect metrics (F1-Score: 1.00), indicating excellent separability and prediction for this class.
- The "Clench Fist" class also performed very well, with an F1-Score of 0.97.
- The "Wrist Flexion" class, while achieving perfect precision (1.00), had slightly lower recall (0.95), suggesting minor room for improvement in capturing all true positives.

Table 3. Validation of the model performances.

	Precision	**Recall**	**F1-Score**
Clench Fist	95%	1	0.97
Wrist Extension	100%	1	1
Wrist Flexion	100%	0.95	0.97

To optimize the training process and improve efficiency, it is essential to address both underfitting and overfitting. One method is to fine-tune the batch size, which determines the number of samples used to update the model's weights in each iteration. Given this study's limited number of available samples, using a maximum batch size (i.e., batch size = total number of acquisitions) is recommended. Additionally, selecting a more advanced optimizer can enhance performance. The Adam optimizer is chosen in our case, as it is widely regarded as one of the most effective optimizers in the current literature [41].

Key hyperparameters such as the learning rate and decay—representing the step size at each iteration—can be adjusted for better precision. While smaller learning rates improve accuracy by taking smaller steps, they also slow down the learning process. Another option is to normalize the input data between 0 and 1 to maintain consistent magnitudes. However, this normalization may slightly slow down the execution on the microcontroller, as each acquisition would require a division operation.

To evaluate the model's performance, 100 consecutive training sessions were conducted. Figure 12 illustrates the accuracy and loss metrics as a function of training iterations. The model quickly converges after approximately 10 sessions, achieving accuracy close to 98%. The model demonstrates strong performance for the three target movements, showing correct behavior and minimal loss.

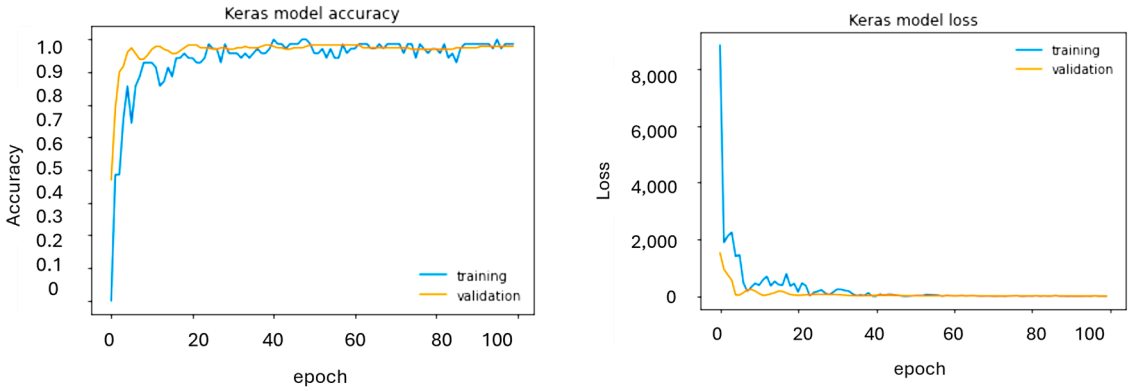

Figure 12. Plot of the accuracy and losses of the processed data using the Keras model.

The model was trained with four more users by using MyoWare sEMG sensors MyoWare AT-04-001 model for holding a bottle and pointing a finger. The obtained signals were processed, and the ANN was applied. One hundred consecutive training sessions were carried out. The results of the training and classification of the signals showed that the model converged around the 50th training session (Figure 13). After converging, the model accuracy is closer to 90%. This accuracy was observed consistently across all users, demonstrating the method's reliability. Compared to the OYMotion sEMG sensor, the accuracy is lower. This accuracy also depends on the recorded signal obtained from the Sparkfun and OYMotion's EMG sensors. This difference can be seen in Figure 6, where it clearly can be perceived that the signal-to-noise ratio of the OYMotion sEMG sensor is significantly higher than that of the MyoWare sEMG sensor.

The system can differentiate the type of movement performed with correct reliability with 80% accuracy. To obtain such precision, it is, however, necessary that the movement be carried out identically as during the learning phase. The neural network model exhibits excellent performance, achieving a holdout accuracy of 98% and an average cross-validation accuracy of 97.33% with low variability ($\pm$1.33%). It demonstrates robustness and balanced class performance, with high precision and recall across all categories. However, a slightly lower recall (0.95) for the "Wrist Flexion" class suggests occasional false negatives and variability in one cross-validation fold (95.00% accuracy) indicates potential sensitivity to data splits. Despite these minor weaknesses, the model's strong generalization and reliability make it suitable for real-world applications such as bionic hand control.

Following neural network improvements, the system was tested under real-world conditions. The results were highly satisfactory, achieving a reliability rate of 95%. The system is resilient to parasitic arm movements and performs best when distinct movements are made, as shown in Figures 14 and 15. This level of reliability ensures the bionic hand

can effectively interpret and execute commands, providing users with a responsive and reliable tool for various tasks.

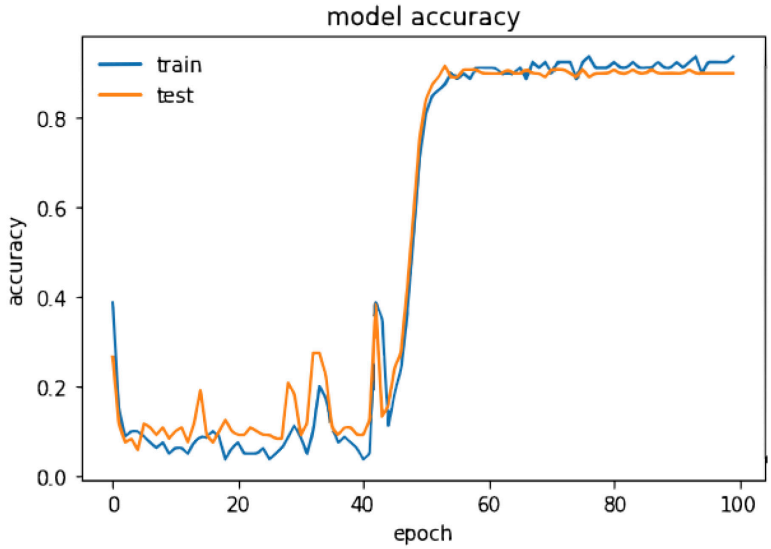

Figure 13. Accuracy results by using MyoWare sEMG sensors MyoWare AT-04-001 model for holding a bottle and pointing a finger.

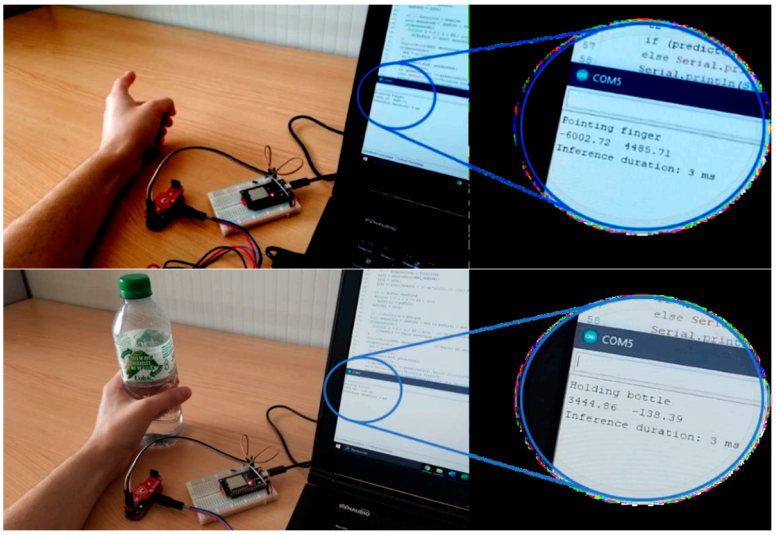

Figure 14. Final test results by using MyoWare sEMG sensors and ANN.

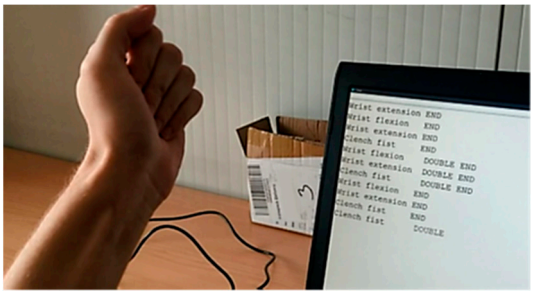

Figure 15. The final test of the system with OYMotion sensors.

Comparatively, in [31], the signal classification using Short-Time Fourier Transform (STFT) achieved an accuracy of 94.8% for a single subject and 76.4% for multiple subject classifications. Similarly, Afroza et al. [42] analyzed feature extraction algorithms in the Frequency Domain (FD), Time Domain (TD), and Time-Frequency Domain (TFD). The

Artificial Neural Network (ANN) yielded the highest accuracy, reaching 97.4%, 0.6% lower than our ANN used in the experiment. In the future, we plan to test algorithms with amputees to define the system accuracy with amputee hands for its use for prosthetic bionic hands. We will evaluating whether the time since amputation affects classification accuracy and system performance.

This strategy will allow us to better understand how to adapt technology to meet the needs of individuals with diverse profiles, making the design more inclusive and functional.

The dataset used for training comprised over 200 signals per gesture. In comparison, prior studies utilized different approaches: for instance, [43] employed data from 40 users, each contributing one signal per gesture, while [44] recorded signals from 10 users. In our study, data were collected from two users, with each contributing 100 signals per gesture, resulting in a total of 600 signals across three gestures.

As demonstrated by studies such as [45] on EMG signal processing, high-quality, consistent data with clear signal separation can be sufficient to train models without the need for data augmentation or extensive regularization techniques.

The integration of a double-trigger mechanism substantially enhances the versatility of the bionic hand, enabling a wider array of movements while maintaining simplicity in the underlying artificial intelligence. This advancement marks a significant progression in the development of more adaptable and user-friendly prosthetic devices. By allowing users to access additional functionalities without increasing system complexity, the double-trigger mechanism improves the overall user experience and provides greater control and flexibility in operating the bionic hand.

The computational efficiency metrics derived from the neural network model are as follows:

- Total training time: 9.81 s;
- Average time per epoch: 0.10 s;
- Average inference time per sample: 0.000676 s.

These results highlight the model's computational efficiency, confirming its suitability for resource-constrained environments and real-time applications such as bionic hand control.

In the current state, the algorithms of filtering, detection and classification by artificial intelligence use 18% of CPU resources, 16% of flash memory and 26% of RAM. The rest of the resources can be used to control the motors and communicate with the user.

4. Conclusions

In this paper, we present a study on processing surface EMG sensor signals for a prosthetic hand designed considering the human hand anatomy. The sEMG sensors detect electrical activity in the muscles, which is then transformed into hand gestures for the prosthetic device. We applied band-pass filters to amplify, filter, and sample these signals for gesture processing. Subsequently, a neural network is employed for pattern recognition and classification. The study involves training the system with signals for hand movements, such as handling a bottle and pointing a finger, while also examining wrist flexion, wrist extension, and fist clenching. The model converges after 10 sessions, achieving 98% accuracy. In total, five movements are analyzed, resulting in an impressive system accuracy of 95%. These results suggest that offline classification can be enhanced and further tested with a real prosthetic hand. Additionally, the findings confirm that high-quality results can be achieved with low-cost technology. Incorporating sensors that measure finger pressure and sensory feedback could provide supplementary input patterns, aiding the classifier in distinguishing gestures more accurately and intuitively.

Author Contributions: Conceptualization, L.D.; methodology, L.D.; software, D.T.; validation, L.D. and I.S.V.; formal analysis, V.B.; investigation, L.D.; resources, V.B.; data curation, I.S.V.; writing—original draft preparation, L.D.; writing—review and editing, I.S.V.; visualization, D.T.; supervision, L.D.; project administration, L.D.; funding acquisition, L.D. All authors have read and agreed to the published version of the manuscript.

Funding: This research was funded by Universitat Politécnica de Valencia.

Institutional Review Board Statement: Not applicable.

Informed Consent Statement: Not applicable.

Data Availability Statement: Data is unavailable due to privacy and database improvement.

Conflicts of Interest: The authors declare no conflict of interest.

References

1. Dunai, L.; Novak, M.; Lengua, I. Development of a prosthetic hand based on human hand anatomy. In Proceedings of the IECON 2020 The 46th Annual Conference of the IEEE Industrial Electronics Society, Singapore, 18–21 October 2020; pp. 600–605. [CrossRef]
2. Erin, M. The New Hero of Upper Limb Prosthetics. Biology: Student Scholarship & Creative Works. 2018. Available online: https://digitalcommons.augustana.edu/biolstudent/18 (accessed on 26 September 2024).
3. Feix, T.; Romero, J.; Ek, C.H.; Schmiedmayer, H.B.; Kragic, D.A. Metric for Comparing the Anthropomorphic Motion Capability of Artificial Hands. Robotics. *IEEE Trans. Robot.* **2013**, *29*, 82–93. [CrossRef]
4. Luchetti, M.; Cutti, A.; Verni, G.; Sacchetti, R.; Rossi, N. Impact of Michelangelo prosthetic hand: Findings from a crossover longitudinal study. *J. Rehabil. Res. Dev.* **2015**, *52*, 605–618. [CrossRef] [PubMed]
5. Chen, Z.; Min, H.; Wang, D.; Xia, Z.; Sun, F.; Fang, B.A. Review of Myoelectric Control for Prosthetic Hand Manipulation. *Biomimetics* **2023**, *8*, 328. [CrossRef] [PubMed]
6. Ottobock Sensor 13E200. Available online: http://www.ottobock.com/ (accessed on 26 September 2024).
7. Mano Michelangelo. Available online: https://www.ottobock.com/es-es/product/8E500 (accessed on 26 September 2024).
8. Sensor Hand. Mano mioeléctrica VariPlus Speed. Available online: https://www.ottobock.com/es-es/product/8E38~59 (accessed on 26 September 2024).
9. Connolly, C. Prosthetic hands from Touch Bionics. *Ind. Robot. Int. J.* **2018**, *35*, 290–293. [CrossRef]
10. VinCent Systems. 2024. Available online: http://handprothese.de/vincent-hand/ (accessed on 26 September 2024).
11. Prosthetic Hands from VINCENT Systems: A lightweight Featuring High-Tech Quality and a Sense of Touch. Available online: https://www.rehacare.com/en/business/Prosthetic-hand-VINCENT-System-lightweight-high-tech-quality-sense-of-touch (accessed on 26 September 2024).
12. Tawfik, M.A.; Baqer, I.A.; Abdulsahib, A.D. Grasping Force Controlling by Slip Detection for Specific Artificial Hand (ottobock 8E37). *Eng. Technol. J.* **2018**, *36*, 979–984. [CrossRef]
13. Bradberry, T.J.; Gentili, R.J.; Contreras-Vidal, J.L. Reconstructing Three-Dimensional Hand Movements from Noninvasive Electroencephalographic Signals. *J. Neurosci.* **2010**, *30*, 3432–3437. [CrossRef]
14. Bundy, D.T.; Pahwa, M.; Szrama, N.; Leuthardt, E.C. Decoding three-dimensional reaching movements using electrocorticographic signals in humans. *J. Neural. Eng.* **2016**, *13*, 026021. [CrossRef]
15. Benatti, S.; Farella, E.; Benini, L.; Gruppioni, E. Analysis of robust implementation of an EMG pattern recognition based control. In Proceedings of the International Conference on Bio-Inspired Systems and Signal Processing-Volume 0BIOSTEC, Angers, France, 3–6 March 2014; pp. 45–54. [CrossRef]
16. Tchantchane, R.; Zhou, H.; Zhang, S.; Alici, G. A Review of Hand Gesture Recognition Systems Based on Noninvasive Wearable Sensors. *Adv. Intell. Syst.* **2023**, *5*, 2300207. [CrossRef]
17. Dario, P.; Micera, S.; Zecca, M. Control of Multifunctional Prosthetic Hands by Processing the Electromyographic Signal. *Crit. Rev. Biomed. Eng.* **2002**, *30*, 459–485. [CrossRef]
18. Barbabas, J.; Radil, R.; Snajdarova, M. Proof of concept EMG-controlled prosthetic hand system–an overview. In Proceedings of the 19th International Conference Computational Problems of Electrical Engineering, Banska Stiavnica, Slovakia, 9–12 September 2018. [CrossRef]
19. Asif, A.R.; Waris, A.; Gilani, S.O.; Jamil, M.; Ashraf, H.; Shafique, M.; Niazi, I.K. Performance Evaluation of Convolutional Neural Network for Hand Gesture Recognition Using EMG. *Sensors* **2020**, *20*, 1642. [CrossRef]
20. Dunai, L.; Novak, M.; García Espert, C. Human Hand Anatomy-Based Prosthetic Hand. *Sensors* **2021**, *21*, 137. [CrossRef]

21. Sartori, M.; Durandau, G.; Doen, S.; Farina, D. Robust simultaneous myoelectric control of multiple degrees of freedom in wrist-hand prostheses by real-time neuromusculoskeletal modeling. *J. Neural Eng.* **2018**, *15*, 066026. [CrossRef] [PubMed]
22. Ghailassi, I.E.; Hashim, N.A.B.; Razak, N.A.A.; Osman, N.A.; Gholizadeh, H.; Astuti, S.D. Investigation of EMG Parameters for Transtibial Amputees While Treadmill Walking with Different Speeds: A Preliminary Study. *IEEE Access* **2024**, *12*, 27356–27367. [CrossRef]
23. Hudgins, B.; Parker, P.; Scott, R. A new Strategy for multifunction myoelectric control. *IEEE Trans. Biomed. Eng.* **1993**, *40*, 82–94. [CrossRef]
24. Englehart, K.; Hudgins, B. A robust, real-time control scheme for multifunction myoelectric control. *IEEE Trans. Biomed. Eng.* **2003**, *50*, 848–854. [CrossRef]
25. Pires, R.; Falcari, T.; Campo, A.B.; Pulcineli, B.C.; Hamill, J.; Ervilha, U.F. Using a Support Vector Machine Algorithm to Classify Lower-Extremity EMG Signals During Running Shod/Unshod With Di_erent Foot Strike Patterns. *J. Appl. Biomech.* **2019**, *35*, 87–90. [CrossRef]
26. Gupta, R.; Agarwal, R. Single channel EMG-based continuous terrain identification with simple classifier for lower limb prosthesis. *Biocybern. Biomed. Eng.* **2019**, *39*, 775–788. [CrossRef]
27. Xie, H.-B.; Guo, T.; Bai, S.; Dokos, S. Hybrid soft computing systems for electromyographic signals analysis: A review. *BioMed Eng OnLine* **2014**, *13*, 1–8. [CrossRef]
28. Prasad, C.; Balakandan, V.K.; Moorthy, P.; Kochuvila, S. Classification of sEMG Signals for Controlling of a Prosthetic foot using SVM and KNN. In Proceedings of the 2019 International Conference on Intelligent Computing and Control Systems (ICCS), Madurai, India, 15–17 May 2019; pp. 454–458. [CrossRef]
29. Meng, M.; Luo, Z.; She, Q.; Ma, Y. Automatic recognition of gait mode from EMG signals of lower limb. In Proceedings of the 2010 The 2nd International Conference on Industrial Mechatronics and Automation, Hong Kong, China, 30 May 2010; pp. 282–285. [CrossRef]
30. Morbidoni, C.; Principi, L.; Mascia, G.; Strazza, A.; Verdini, F.; Cucchiarelli, A.; Di Nardo, F. Gait phase classification from surface EMG signals using Neural Networks. In *Mediterranean Conference on Medical and Biological Engineering and Computing*; Springer: Cham, Switzerland, 2019; pp. 75–82. [CrossRef]
31. Mesbah, S.; Gonnelli, F.; El-baz, A.; Angeli, C.; Harkema, S.; Rejc, E. Spectral analysis of lower limb EMG activity in individuals with motor complete SCI during standing with epidural stimulation. In Proceedings of the 2018 IEEE International Symposium on Signal Processing and Information Technology (ISSPIT), Louisville, KY, USA, 6–8 December 2018; pp. 1–5. [CrossRef]
32. Asghar, A.; Jawaid Khan, S.; Azim, F.; Shakeel, C.S.; Hussain, A.; Niazi, I.K. Review on electromyography based intention for upper limb control using pattern recognition for human-machine interaction. *Proc. Inst. Mech. Eng. Part H J. Eng. Med.* **2022**, *236*, 628–645. [CrossRef]
33. Ng, A.; Katanforoosh, K.; Besouda Mourri, Y. Deep Learning Specialization. 2020. Available online: https://www.deeplearning.ai/ (accessed on 26 September 2024).
34. Srivastava, N.; Hinton, G.; Krizhevsky, A.; Sutskever, I.; Salakhutdinov, R. Dropout: A simple way to prevent neural networks from overfitting. *J. Mach. Learn. Res.* **2014**, *15*, 1929–1958.
35. Zaidi, S.A.; Hayajneh, A.M.; Hafeez, M.; Ahmed, Q.Z. Unlocking Edge Intelligence Through Tiny Machine Learning (TinyML). *IEEE Access* **2022**, *10*, 100867–100877. [CrossRef]
36. Wei, L.; Ping, S.; Hongliu, Y. Gesture Recognition Using Surface Electromyography and Deep Learning for Prostheses Hand: State-of-the-Art, Challenges, and Future. *Front. Neurosci.* **2021**, *15*, 1–20. [CrossRef]
37. Fedorov, I.; Stamenovic, M.; Jensen, C.; Yang, L.-C.; Mandell, A.; Gan, Y.; Mattina, M.; Whatmough, P.N. TinyLSTMs: Efficient Neural Speech Enhancement for Hearing Aids. In Proceedings of the 21st Interspeech International Conference, Shanghai, China, 25–29 October 2020; pp. 4054–4058. [CrossRef]
38. Alajlan, N.N.; Ibrahim, D.M. TinyML: Enabling of Inference Deep Learning Models on Ultra-Low-Power IoT Edge Devices for AI Applications. *Micromachines* **2022**, *13*, 851. [CrossRef] [PubMed]
39. Kumari, A.K.; Bhatt Dwivedi, R.K.; Belwal, R. Accuracy Testing of Data Classification using Tensor Flow a Python Framework in ANN Designing. In Proceedings of the 2018 International Conference on System Modeling & Advancement in Research Trends (SMART), Moradabad, India, 23–24 November 2018; pp. 44–48. [CrossRef]
40. Venzke, M.; Klisch, D.; Kubik, P.; Ali, A.; Missier, J.D.; Turau, V. Artificial Neural Networks for Sensor Data Classification on Small Embedded Systems. *arXiv* **2020**, arXiv:2012.08403v1.
41. Huttunen, H. Deep Neural Networks: A Signal Processing Perspective. In *Handbook of Signal Processing Systems*; Bhattacharyya, S., Deprettere, E., Leupers, R., Takala, J., Eds.; Springer: Cham, Switzerland, 2019. [CrossRef]
42. Sultana, A.; Ahmed, F.; Alam, M.S. A systematic review on surface electromyography-based classification system for identifying hand and finger movements. *Healthc. Anal.* **2023**, *3*, 100–126. [CrossRef]
43. Ozdemir, M.A.; Kisa, D.H.; Guren, O.; Akan, A. Dataset for multi-channel surface electromyography (sEMG) signals of hand gestures. *Data Brief* **2022**, *4*, 107921. [CrossRef]

44. Li, S.; Sun, W.; Li, W.; Yu, H. Enhancing Robustness of Surface Electromyography Pattern Recognition at Different Arm Positions for Transhumeral Amputees Using Deep Adversarial Inception Domain Adaptation. *Appl. Sci.* **2024**, *14*, 3417. [CrossRef]
45. Tsinganos, P.; Cornelis, B.; Cornelis, J.; Jansen, B.; Skodras, A. Data Augmentation of Surface Electromyography for Hand Gesture Recognition. *Sensors* **2020**, *20*, 4892. [CrossRef]

Disclaimer/Publisher's Note: The statements, opinions and data contained in all publications are solely those of the individual author(s) and contributor(s) and not of MDPI and/or the editor(s). MDPI and/or the editor(s) disclaim responsibility for any injury to people or property resulting from any ideas, methods, instructions or products referred to in the content.